Acta Neuropathol (Berl) (1983) 60:257–265

Acta Neuropathologica

Oligodendrocyte Infection and Demyelination Produced in Mice by the M9 Mutant of Semliki Forest Virus*

B. J. Sheahan[1], M. C. Gates[2], J. F. Caffrey[1], G. J. Atkins[2]

[1] Dept. of Veterinary Pathology and Microbiology, Veterinary College of Ireland, Ballsbridge, Dublin 4, Republic of Ireland
[2] Dept. of Microbiology, Trinity College, Dublin 2, Republic of Ireland

Summary. Intraperitoneal inoculation with the M9 mutant of Semliki Forest virus caused focal demyelinating encephalomyelitis in weanling BALB/c and C57BL/6 mice. Demyelination was more severe in BALB/c than in C57BL/6 mice. Virus particles were seen in oligodendrocytes in areas of myelin vacuolation 5 and 7 days post inoculation (DPI). Oligodendrocytes containing virus in BALB/c mice showed hypertrophy and vacuolar degeneration. There was a mononuclear cell infiltrate and lymphocytes and necrotic cells were present in vacuoles in myelin sheaths. Demyelinating plaques containing macrophages laden with myelin debris were most prominent 14 DPI when virus was cleared from the brain. Remyelination of the central type occurred 28 DPI in BALB/c mice. These findings indicate that direct virus-induced injury to oligodendrocytes has a major role in the initiation of inflammation and demyelination in this model system.

Key words: Semliki Forest virus – Oligodendrocytes – Demyelination – Remyelination

Introduction

Semliki Forest virus (SFV) is a neurotropic alphavirus which has been extensively used for laboratory studies of pathogenicity. Many strains of SFV have been isolated but most attention has been paid to virulent strains which cause a fatal encephalitis in all groups of mice and to an avirulent strain (A774) which causes demyelination in weanling mice but without death and rarely with clinical signs (Chew-Lim 1975; Chew-Lim et al. 1977; Pathak et al. 1976; Pathak and Webb 1978). It has been suggested that the demyelination in A774 infected mice is immunologically mediated (Jagelman et al. 1978; Suckling et al. 1978; Berger 1980; Kelly et al. 1982).

As part of a study of the pathogenicity of SFV we isolated four neurovirulence mutants of a highly virulent wild-type (wt) strain after mutagenesis and screening (Barrett et al. 1980). These mutants allowed survival of most i.p. infected mice at doses which were lethal for the wt virus. Demyelination occurred in 35% of weanling mice after i.p. inoculation with 10^2 p.f.u. of the mutant M136 (Sheahan et al. 1981). Virus was seen in necrotic cells putatively identified as oligodendrocytes, and we suggested that the demyelination followed the selective destruction of these cells. We have subsequently found that the mutant M9 is a better model for the study of demyelination, since lesions of acute demyelinating encephalomyelitis were detected in 94% of mice infected with this mutant. Virus particles were present in cells which could be identified as oligodendrocytes, and a rapid cytopathic effect was produced in G26-24 (oligodendroglioma) cells after low levels of viral RNA synthesis (Atkins and Sheahan 1982). Ultrastructural studies of infected G26-24 cells have shown severe cytolytic changes in the presence of small numbers of virus particles (unpublished data).

In this paper we present details of morphological changes in the central nervous system (CNS) of weanling mice infected with the mutant M9. We describe differences in the response of BALB/c and C57BL/6 mice infected with this virus. The findings support the suggestion that the oligodendrocyte is the primary CNS target in this disease.

Materials and Methods

Virus

The isolation and characterization of the M9 mutant of SFV, and methods for the titration of virus in blood and brain have been described previously (Barrett et al. 1980; Atkins and Sheahan 1982).

* Supported by the Medical Research Council of Ireland
Offprint requests to: Dr. B. J. Sheahan (address see above)

Mice

Because variations in susceptibility to A774 infection have been reported in different strains of mice (Suckling et al. 1980) it was decided to compare the response to M9 infection in inbred BALB/c and C57BL/6 mice. Weanling (30–40-day-old) mice were used throughout, and were inoculated i.p. with 10^3 p.f.u. of virus in 0.3 ml of phosphate-buffered saline.

Morphology

BALB/c mice were killed after 5 days (8 mice), 7 days (3 mice), 14 days (17 mice), 21 days (3 mice), 28 days (14 mice), 56 days (3 mice) and 112 days (3 mice). C57BL/6 mice were killed after 5 days (3 mice), 7 days (3 mice), 14 days (3 mice) and 21 days (2 mice). The mice were anaesthetised with ether and perfused via the left ventricle with 3% glutaraldehyde in phosphate buffer. The optic nerves were removed and coronal slices were cut from the brain and spinal cord as previously described (Sheahan et al. 1981). The tissues were post-fixed in phosphate-buffered osmium tetroxide or in a mixture of buffered osmium tetroxide and 1.5% potassium ferricyanide (Langford and Coggeshall 1980) and embedded in Araldite. One-micrometer sections for light microscopy were stained with toluidine blue. Thin sections for electron microscopy were stained with uranyl acetate and lead citrate.

Coronal sections of the brain at the level of the hippocampus were embedded in paraffin wax, sectioned and stained with haematoxylin-eosin (HE).

Results

Clinical Findings

Most infected mice showed ruffling of the fur, lethargy and paresis beginning 5 DPI. The mortality was 12% in BALB/c and 28.8% in C57BL/6 mice with mean times of death of 10.3 days and 8.9 days, respectively. These differences were not statistically significant ($p > 0.05$). Of the survivors, 28.6% of BALB/c and 30.4% of C57BL/6 mice showed paralysis of one or more limbs. Most infected mice, including many which had shown paralysis earlier, appeared normal by 28 DPI.

Light Microscopy

The severity of lesions in paralysed animals correlated with the severity of clinical signs but many clinically silent lesions were also found. Lesions were randomly distributed at all levels including the optic nerves and were more prominent in the spinal cord than in the brain. Within the spinal cord lesions occurred most frequently at the entry and exit zones of spinal nerve roots.

BALB/c Mice. Focal areas of spongy change with myelin vacuolation were common in grey and white

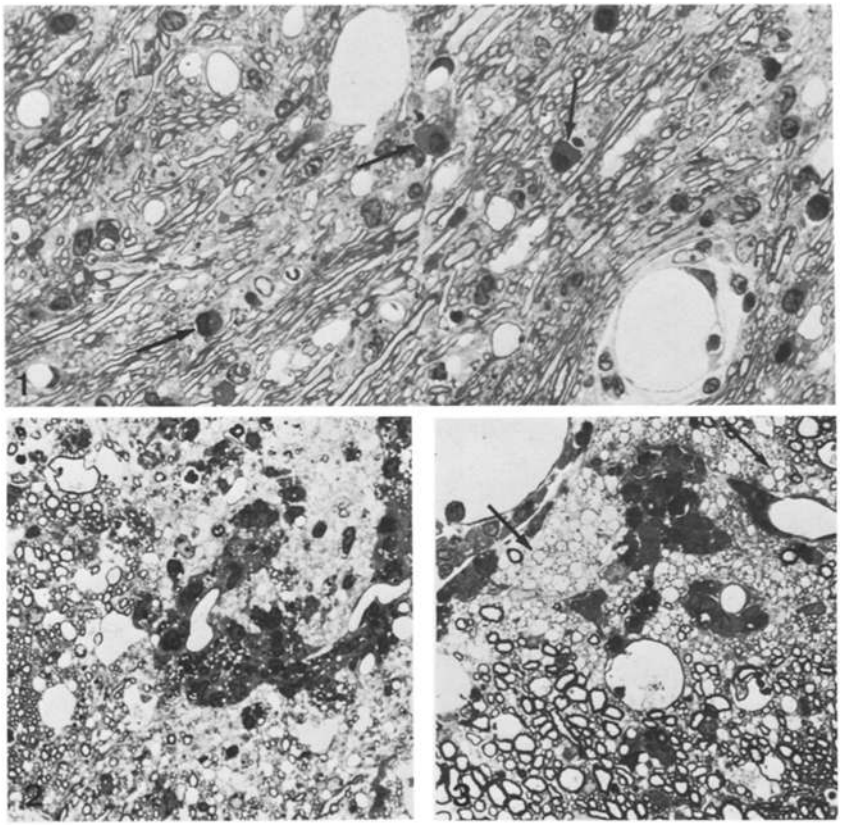

Fig. 1. BALB/c mouse, mid-brain, 5 DPI. Myelin vacuolation, mononuclear cell infiltration and hypertrophic oligodendrocytes (*arrows*). Toluidine blue, ×1,200

Fig. 2. BALB/c mouse, spinal cord, 14 DPI. Demyelinated plaque with myelin vacuoles and macrophages laden with lipid vacuoles and myelin debris. Toluidine blue, ×1,200

Fig. 3. BALB/c mouse, spinal cord, 28 DPI. Myelin vacuoles, mononuclear leucocytes, macrophages with myelin debris and remyelinating axons (*arrows*). Toluidine blue, ×1,200

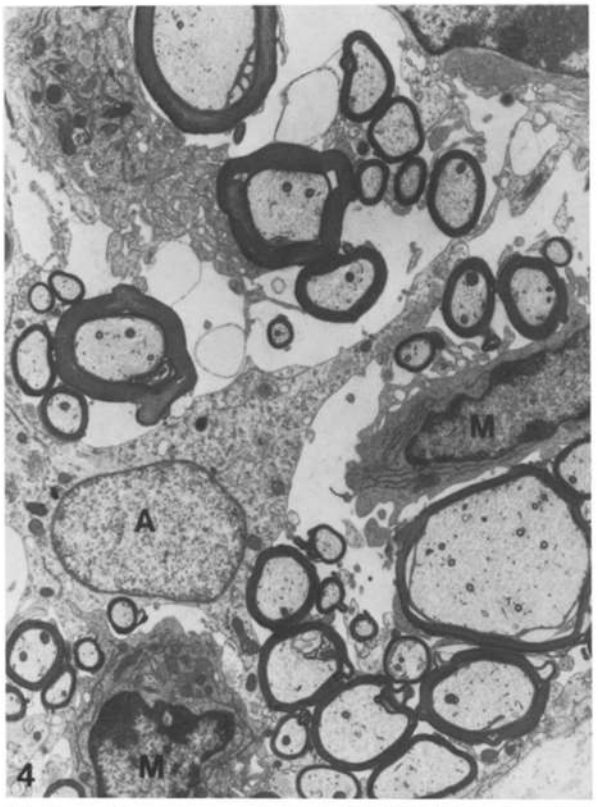

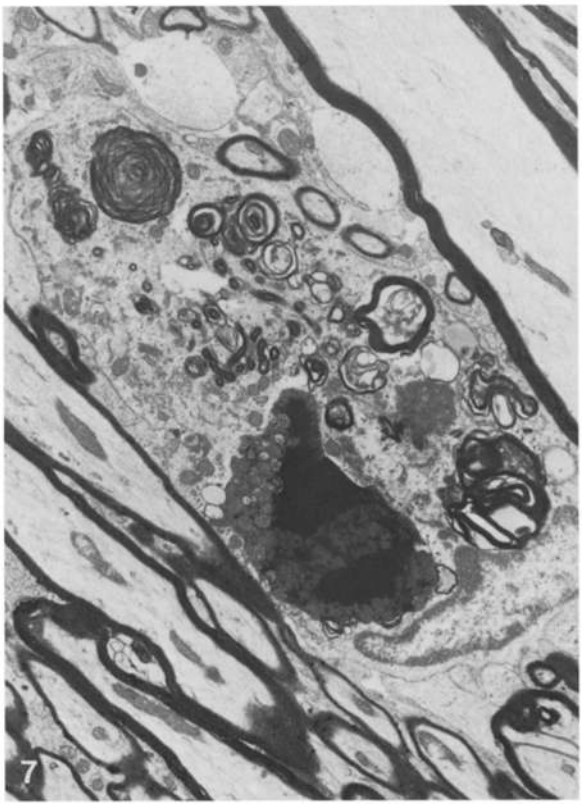

Fig. 4. BALB/c mouse, spinal cord, 5 DPI. Macrophages (*M*) and increased extracellular space around an astrocyte (**A**). ×6,060

Fig. 5. BALB/c mouse, spinal cord, 5 DPI. Vacuolation and vesicular disruption of myelin with necrotic cell debris (*D*). Proliferative changes in the axon at bottom. ×9,380

Fig. 6. BALB/c mouse, spinal cord, 7 DPI. Necrotic cell surrounded by outermost lamellae of a myelin sheath. ×18,000

Fig. 7. BALB/ mouse, mid-brain, 5 DPI. Myelin debris and a necrotic cell in the cytoplasm of a macrophage. ×7,255

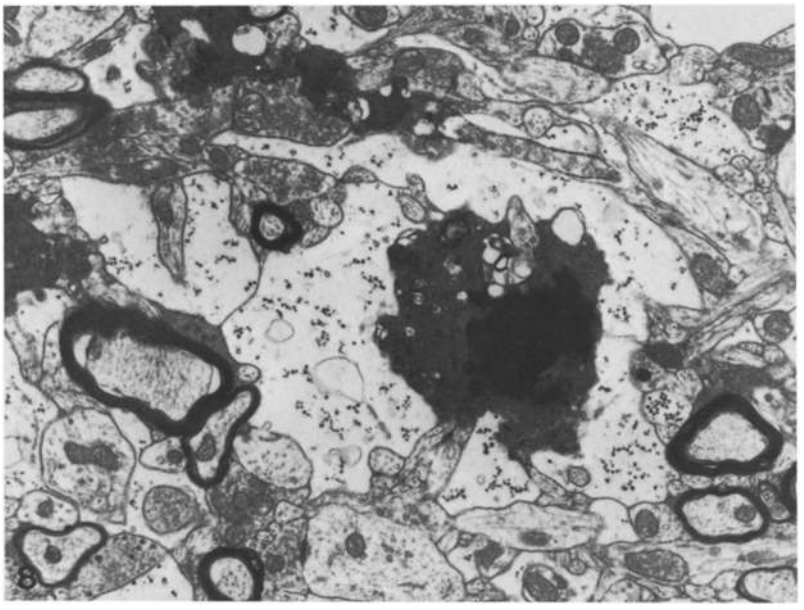

Fig. 8. BALB/c mouse, mid-brain, 5 DPI. Vacuolated astrocyte processes around a necrotic cell. ×13,020

matter 5 and 7 DPI. Cells resembling hypertrophic oligodendrocytes with eccentric nuclei and dense cytoplasm were seen in some areas of myelin vacuolation (Fig. 1). Mononuclear leucocytes were present in the neuropil and associated with blood vessels in the neuropil and leptomeninges. Necrotic cells with dense pycnotic nuclei adjoined myelin vacuoles and apparently normal myelinated axons. Focal areas of myelin pallor and vacuolation with macrophages containing myelin debris were seen 14 DPI (Fig. 2). Most axons appeared normal although a few were seen to undergo Wallerian degeneration in the more severely affected areas. Deposits of myelin debris and necrotic cells were present in these lesions and also randomly distributed in otherwise normal white matter. Macrophages distended with lipid droplets and myelin debris were prominent 21 and 28 DPI. Remyelinating axons with thinner than normal myelin sheaths were seen in areas of myelin pallor 28 DPI (Fig. 3). Cells with pycnotic nuclei were unusual at this stage. The only changes seen 56 and 112 DPI were isolated deposits of myelin debris in the white matter of the spinal cord.

C57BL/6 Mice. Spongy change was less severe, and necrosis was more prominent at all intervals after infection than in BALB/c mice. Some mice showed focal necrosis with polymorphonuclear leucocytes 5 and 7 DPI. Inflammation was more extensive 14 DPI but aggregates of naked axons were not seen. Focal areas of necrosis with foamy macrophages and fibrillary gliosis were prominent in grey and white matter 21 DPI.

Electron Microscopy

BALB/c Mice. The appearance of the spongiform lesions 5 DPI was of an increase in extracellular space suggestive of oedema (Fig. 4). Myelin sheaths showed vacuolation and vesicular disruption. Axons mostly appeared normal although some showed accumulation of mitochondria and membranous profiles (Fig. 5). Macrophages and occasional polymorphonuclear leucocytes were seen in the neuropil. Necrotic cells with electron-dense nuclei adjoined or were surrounded by the outermost lamellae of myelin sheaths (Fig. 6). Similar necrotic cells were occasionally seen in the perivascular spaces or engulfed by macrophages (Fig. 7). Astrocytes and astrocytic processes adjoining necrotic cells were vacuolated (Fig. 8). Large oligodendrocytes with eccentric nuclei and extensive cytoplasm containing vacuoles, microtubules, profiles of smooth endoplasmic reticulum and virus particles occurred in areas of myelin vacuolation (Fig. 9a, b). Some of these cells showed connections with vacuolated myelin sheaths. The virus particles occurred mostly as nucleocapsids about 25 nm in diameter. Mature virus particles about 40 nm in diameter were present in cytoplasmic vacuoles (Fig. 9c). Occasionally, virus particles were seen in the extracellular space adjoining infected oligodendrocytes and in the cytoplasm of some necrotic cells.

The lesions 7 DPI were similar except that oligodendrocytes containing virus particles were more difficult to find. Occasional lymphocytes with extensive cytoplasm containing free ribosomes were seen in vacuoles in

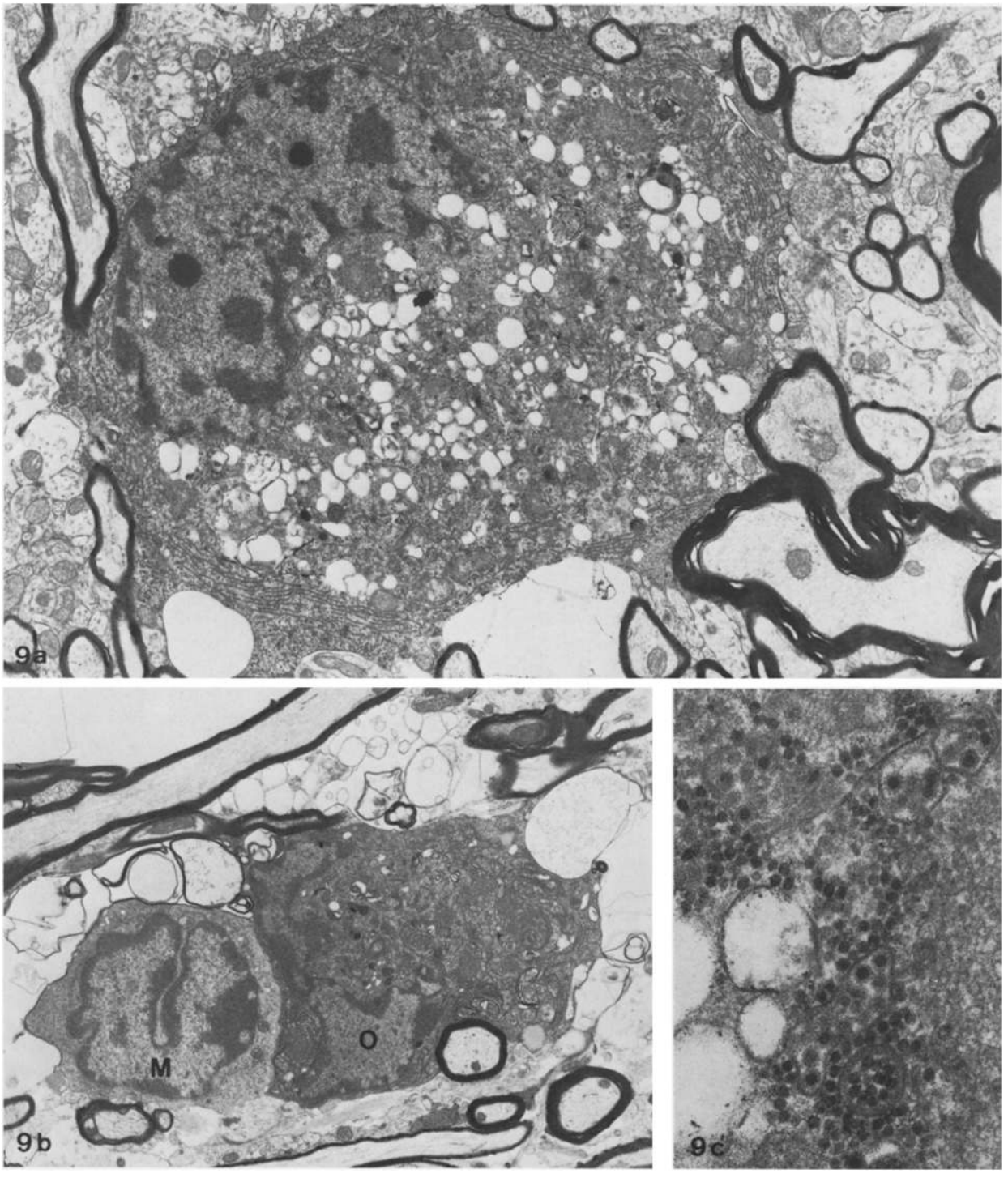

Fig. 9a–c. Detail from Fig. 1. **a** Hypertrophic oligodendrocyte with eccentric nucleus and vacuoles, proliferated smooth endoplasmic reticulum and virus particles in the cytoplasm. ×14.210. **b** Hypertrophic oligodendrocyte (*O*) and a macrophage (*M*) in an area of myelin vacuolation. ×8,465. **c** Higher magnification of oligodendrocyte cytoplasm in **a**. Vacuoles, mature virus particles and virus nucleocapsids. ×68,000

myelin sheaths (Fig. 10). Similar cells were seen in myelin sheaths 14 DPI. The myelin sheaths invaded by lymphocytes otherwise appeared normal or showed vacuolar change (Fig. 11). At 14 DPI aggregates of naked axons were seen in glial-free areas closely associated with macrophages containing myelin debris (Fig. 12). Macrophage processes extended around many myelinated axons showing vacuolation and

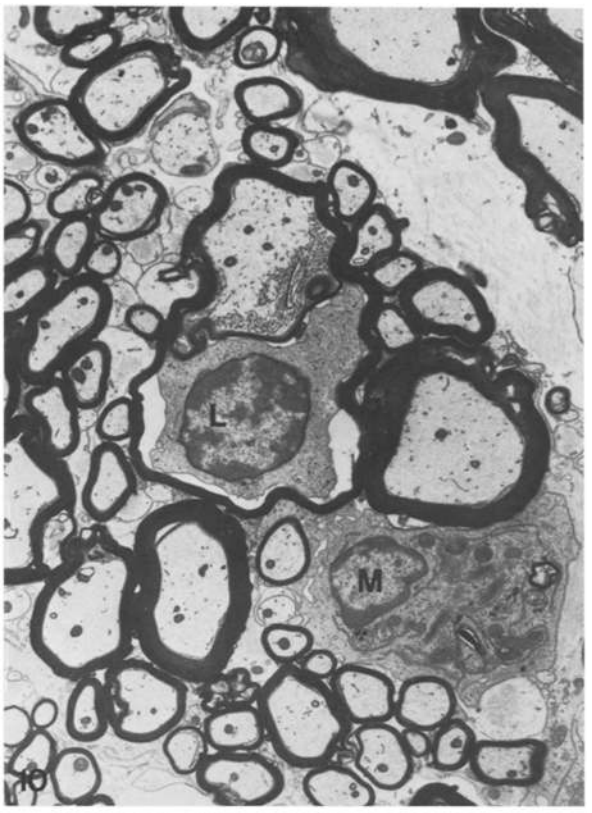

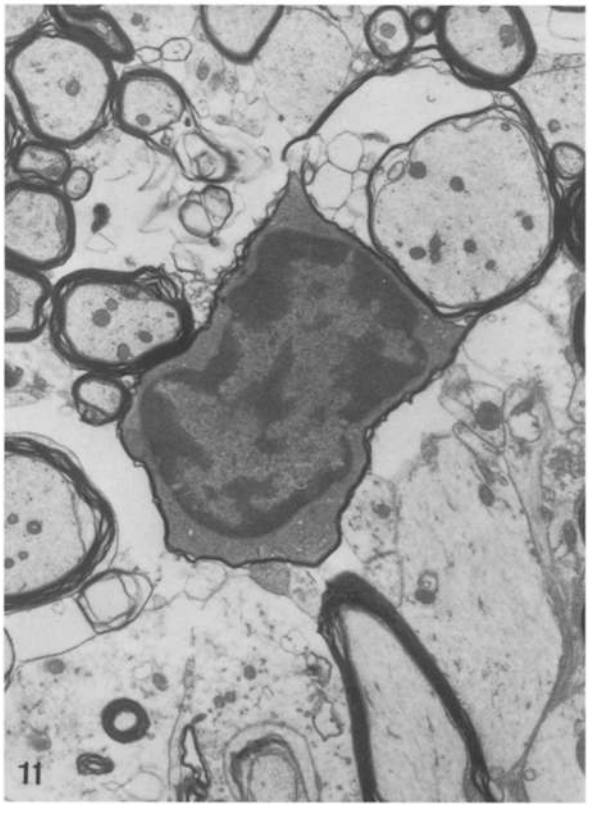

Fig. 10. BALB/c mouse, spinal cord, 5 DPI. A lymphocyte (*L*) in a vacuole in a myelin sheath with proliferative changes in the axon. A macrophage (*M*) in the neuropil. × 6,700

Fig. 11. BALB/c mouse, spinal cord, 14 DPI. A lymphocyte in a myelin sheath with vacuolation of the sheath. × 9,800

vesicular disruption of the sheaths. Active stripping of myelin lamellae by macrophages was not seen. Oligodendrocytes appeared normal at this stage, and no virus particles were seen.

Macrophages packed with myelin debris were present in the perivascular spaces 21 and 28 DPI (Fig. 13a). Lymphocytes and occasional plasma cells were present in association with these cells. Remyelination characterized by axons with thinner than normal myelin sheaths and prominent inner tongues of oligodendrocyte cytoplasm was seen 28 DPI (Fig. 13b). Occasional naked axons occurred in areas of remyelination. There was a relative increase in astrocytic processes, and necrotic cells were uncommon. Myelinated axons appeared normal 56 and 112 DPI.

C57BL/6 Mice. Occasional virus particles were seen in oligodendrocytes 5 DPI. Oligodendrocytes otherwise appeared normal with no evidence of hypertrophic or degenerative changes. Macrophages and necrotic cells similar to those in BALB/c mice were common. Naked axons and vacuolated myelin sheaths did not occur with the same frequency as in BALB/c mice.

Virus Titrations

The virus content of blood and brain of groups of six mice was estimated at 7, 14 and 21 DPI. Virus was recovered from the brains of both BALB/c and C57BL/6 mice at 7 DPI where it reached average values of 2.2×10^6 p.f.u./g brain and 11.0×10^6 p.f.u./g brain, respectively. These values were not significantly different ($p > 0.05$). Virus was not recovered from brain at 14 and 21 DPI or from blood at any time tested. Thus, virus had been cleared from the brain by 14 DPI and from the blood by 7 DPI.

Discussion

Our results show that the M9 mutant of SFV multiplied selectively in oligodendrocytes in both strains of weanling mice studied. The cytolytic effect of virus multiplication on oligodendrocytes initiated an acute inflammatory demyelinating reaction which was followed by remyelination. Demyelination occurred to a greater degree in BALB/c than in C57BL/6 mice.

Direct virus damage to oligodendrocytes and the host-immune response have been recognised as factors leading to demyelination in experimental models of virus-induced demyelinating disease. The relative importance of these factors in different models has been the subject of intensive investigation (Wisniewski 1977; Dal Canto and Rabinowitz 1982). The best studied

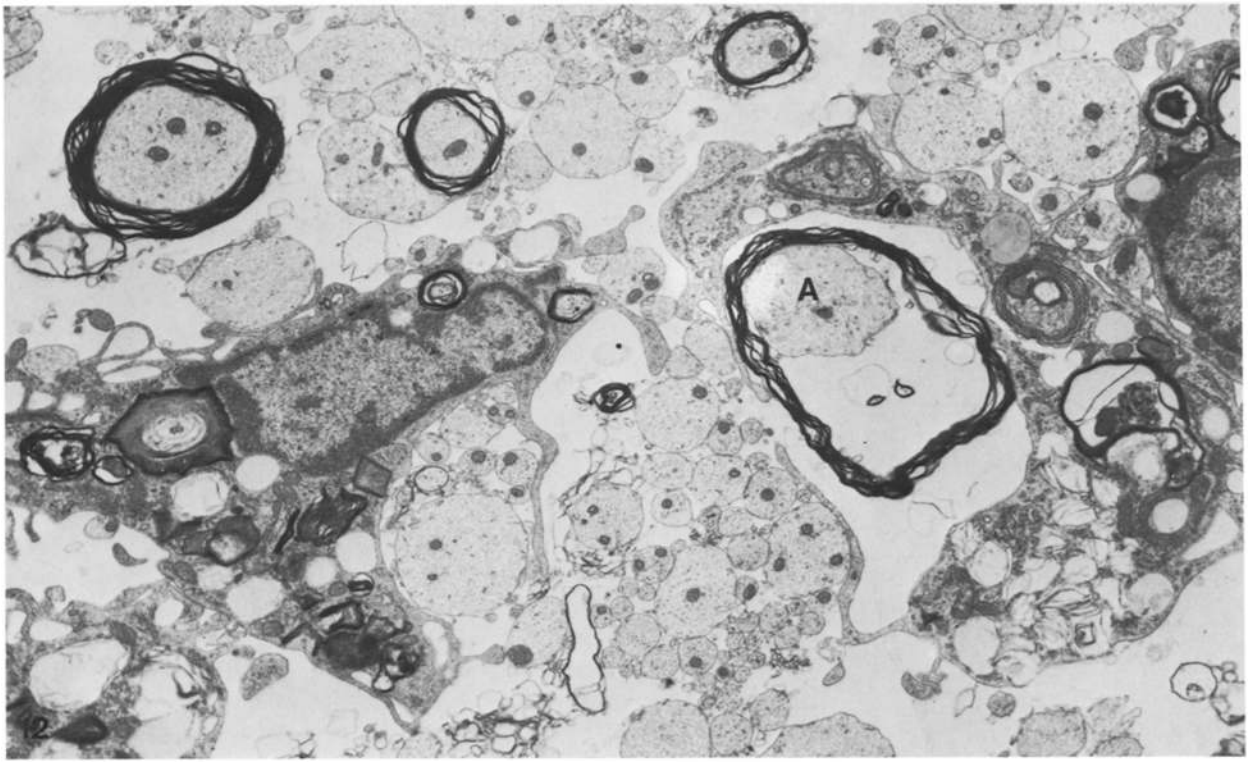

Fig. 12. BALB/c mouse, spinal cord, 14 DPI. Naked axons, macrophages and myelin debris in a glial-free area. Macrophage processes around an axon (*A*) with a vacuolated myelin sheath. ×9,440

virus producing a cytolytic effect on oligodendrocytes is the JHM strain of mouse hepatitis virus (MHV). JHM-MHV has been shown to produce acute and chronic demyelination in mice (Lampert et al. 1973; Stohlman and Weiner 1981) as well as subacute and late demyelination in rats (Wege et al. 1982). Variations in the type of disease produced by this virus are influenced by the dose of virus, the route of inoculation and the age of the host at the time of infection (Weiner 1973). The virus occurs in ependymal cells, astrocytes, neurones, oligodendrocytes, endothelial cells and cells of haematogenous origin (Fleury et al. 1980). Demyelination in JHM-MHV infected mice appears to be dependent on direct cytopathic effect on oligodendrocytes rather than on the host immune response since immunosuppression enhances the mortality of infected mice but does not inhibit the demyelination (Weiner 1973; Weiner et al. 1973).

In the present study the changes which occurred in mice infected with M9 resembled those reported in JHM-MHV infected mice in that proliferative and degenerative alterations occurred in oligodendrocytes as a result of virus multiplication. The significance of the proliferative changes is not understood. Powell and Lampert (1975) suggested that they may be a non-specific accompaniment of cellular injury or a reflection of changes in the stability of the cells as their processes swell. In contrast to the JHM-MHV model, in which cellular infiltrates were reported as scanty or absent in the early stages (Powell and Lampert 1975), mononuclear leucocytes were prominent in the lesions caused by M9 as early as 5 DPI. These leucocytes occurred in the perivascular spaces, in the parenchyma and in vacuoles in myelin sheaths. Necrotic cells showed a similar distribution suggesting that many were of haematogenous origin. Furthermore, in contrast to the cellular pantropism of JHM-MHV, M9 was found only in oligodendrocytes indicating that selective damage to these cells constituted the stimulus for the leucocyte response in this infection.

Neither virus particles, oligodendrocyte degeneration nor necrotic cells have been reported in mice infected with the avirulent A774 strain of SFV (Chew-Lim 1975; Chew-Lim et al. 1977; Pathak et al. 1976; Pathak and Webb 1978; Kelly et al. 1982). The severity of myelin degeneration in M9 infected mice also appears greater than that reported in the A774 model. Kelly et al. (1982) described lymphocytes in the neuropil in A774 infected mice and concluded from the interaction between these cells and glia that the demyelination probably had an immunological basis. Virological studies showed that maximum demyelination occurred when virus had been cleared from the brain (Jagelman et al. 1978). In the present study

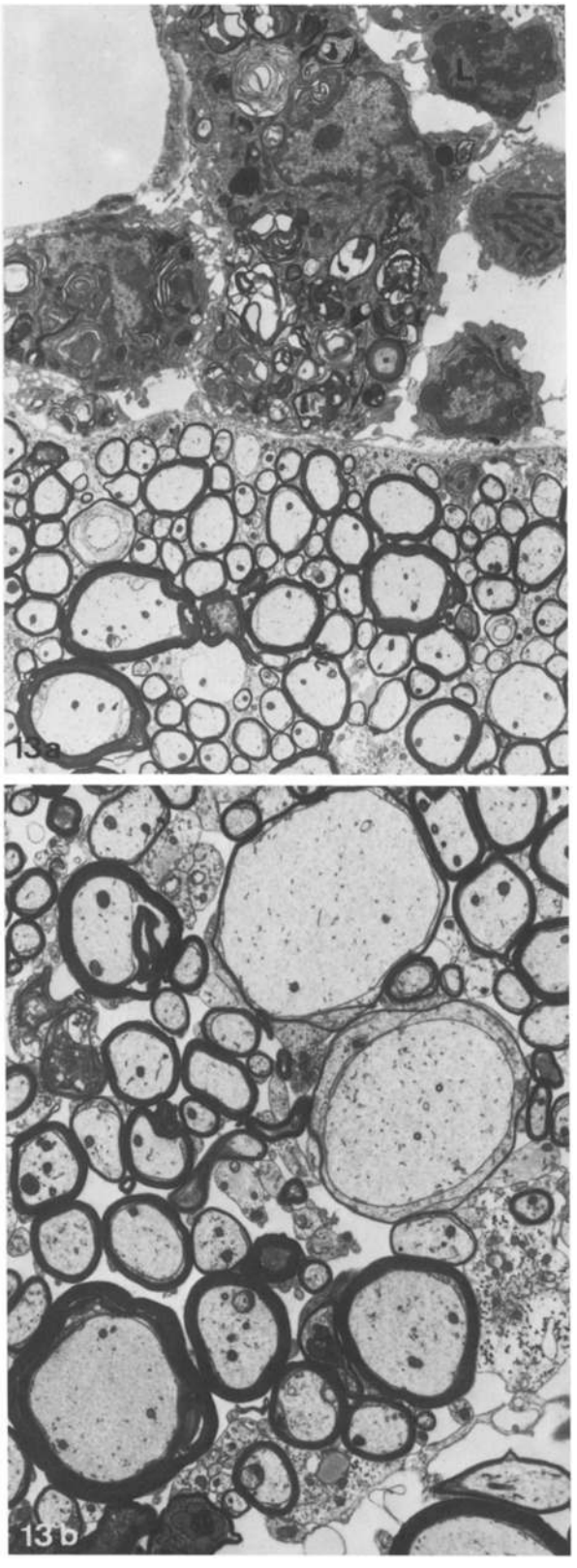

Fig. 13. BALB/c mouse, spinal cord, 28 DPI. **a** Macrophages with myelin debris and a lymphocyte (*L*) in a perivascular space. Many axons have thinner than normal myelin sheaths. ×4,150. **b** Detail of remyelinating axons with thinner than normal myelin sheaths and prominent tongues of oligodendrocyte cytoplasm. ×6,510

demyelination was also most active at a time when virus had been cleared from the brain and the number and location of lymphocytes in the CNS suggested that they, together with macrophages, played major roles in the mechanism of demyelination. It is known that lymphocytes can destroy myelin in vitro (Arnason et al. 1969) and that isolated myelin is vulnerable to attack by neutral proteases secreted by stimulated macrophages (Cammer et al. 1978). The release of soluble products with myelinolytic activity from lymphocytes sensitised to myelin and/or viral antigens could account for the degeneration in some myelin sheaths invaded by lymphocytes in the present study. Similarly, the release of proteases from macrophages could account for the changes seen 14 DPI which suggested that myelin was lysed from affected fibres by macrophages prior to phagocytosis.

The occurrence of remyelination of the central type in M9 infected mice correlated with other models of acute virus-induced demyelination in mice where naked axons are rarely found later than the third week after infection (Stohlman and Weiner 1981). This finding is also consistent with the hypothesis that cells of the oligodendroglial line in mice can regenerate and replace those destroyed by virus infection (Herndon et al. 1977). A few naked axons were seen in areas of remyelination in the present study 28 DPI. Since astrocytes are believed to play an important role in the remyelinating process (Blakemore 1981) it is possible that delayed remyelination of these axons may have reflected the vacuolar degeneration seen in astrocytes during the first week of the disease. The reason for the different responses of BALB/c and C57BL/6 mice to infection with M9 remains to be determined.

This and previous studies have shown infection by the M9 mutant of SFV in BALB/c mice to be an excellent model for the study of virus-induced demyelination and that the trigger for demyelination in this system is destruction of oligodendrocytes. We are presently utilizing a range of immunologically compromised mice to assess the significance of immune mechanisms in the pathogenesis of demyelination in this model.

Acknowledgements. We thank P. Christie for excellent technical assistance, C. King for assistance with photography, P. Wilson for advice on animal management and A. Nardone for typing the manuscript.

References

Arnason BGW, Winkler GF, Hadler NM (1969) Cell-mediated demyelination of peripheral nerve in tissue culture. Lab Invest 21:1–10

Atkins GJ, Sheahan BJ (1982) Semliki Forest virus neurovirulence mutants have altered cytopathogenicity for cells of the central nervous system. Infect Immun 36:333–341

Barrett PN, Sheahan BJ, Atkins GJ (1980) Isolation and preliminary characterization of Semliki Forest virus mutants with altered virulence. J Gen Virol 49:141–147

Berger ML (1980) Humoral and cell-mediated immune mechanisms in the production of pathology in avirulent Semliki Forest virus encephalitis. Infect Immun 30:244–253

Blakemore WF (1981) Remyelination in the CNS. In: Acosta Vidrio E, Fedoroff S (eds). Glial and neuronal cell biology. Eleventh International Congress of Anatomy, part A. Liss, New York, pp 105–109

Cammer W, Bloom BR, Norton WT, Gordon S (1978) Degradation of basic protein in myelin by neutral proteases secreted by stimulated macrophages – a possible mechanism of inflammatory demyelination. Proc Natl Acad Sci USA 75:1554–1558

Chew-Lim M (1975) Mouse encephalitis induced by avirulent Semliki Forest virus. Vet Pathol 12:387–393

Chew-Lim M, Suckling AJ, Webb HE (1977) Demyelination in mice after two or three infections with avirulent Semliki Forest virus. Vet Pathol 14:67–72

Dal Canto MC, Rabinowitz SG (1982) Experimental models of virus – induced demyelination of the central nervous system. Ann Neurol 11:109–127

Fleury HJA, Sheppard RD, Bornstein MB, Raine CS (1980) Further ultrastructural observations of virus morphogenesis and myelin pathology in JHM virus encephalomyelitis. Neuropathol Appl Neurobiol 6:165–179

Herndon RM, Price DL, Weiner LP (1977) Regeneration of oligodendroglia during recovery from demyelinating disease. Science 195:693–694

Jagelman S, Suckling AJ, Webb HE, Bowen ETW (1978) The pathogenesis of avirulent Semliki Forest virus infections in athymic nude mice. J Gen Virol 41:599–607

Kelly WR, Blakemore WF, Jagelman S, Webb HE (1982) Demyelination induced in mice by avirulent Semliki Forest virus. II. An ultrastructural study of focal demyelination in the brain. Neuropathol Appl Neurobiol 8:43–53

Lampert PW, Sims JK, Kniazeff AJ (1973) Mechanism of demyelination in JHM virus encephalomyelitis. Electron-microscopic studies. Acta Neuropathol (Berl) 24:76–85

Langford LA, Coggeshall RE (1980) The use of potassium ferricyanide in neural fixation. Anat Rec 197:297–303

Pathak S, Webb HE, Oaten SW, Bateman S (1976) An electron-microscopic study of the development of virulent and avirulent strains of Semliki Forest virus in mouse brain. J Neurol Sci 28:289–300

Pathak S, Webb HE (1978) An electron-microscopic study of avirulent and virulent Semliki Forest virus in the brains of different ages of mice. J Neurol Sci 39:199–211

Powell HC, Lampert PW (1975) Oligodendrocytes and their myelin-plasma membrane connections in JHM mouse hepatitis virus encephalomyelitis. Lab Invest 33:440–445

Sheahan BJ, Barrett PN, Atkins GJ (1981) Demyelination in mice resulting from infection with a mutant of Semliki Forest virus. Acta Neuropathol (Berl) 53:129–136

Stohlman SA, Weiner LP (1981) Chronic central nervous system demyelination in mice after JHM virus infection. Neurology 31:38–44

Suckling AJ, Pathak S, Jagelman S, Webb HE (1978) Virus-associated demyelination. A model using avirulent Semliki Forest virus infection of mice. J Neurol Sci 39:147–154

Suckling AJ, Jagelman S, Illavia SJ, Webb HE (1980) The effect of mouse strain on the pathogenesis of the encephalitis and demyelination induced by avirulent Semliki Forest virus infections. Br J Exp Pathol 61:281–284

Wege H, Siddell S, ter Meulen V (1982) The biology and pathogenesis of coronaviruses. Curr Top Microbiol Immunol 99:165–200

Weiner LP (1973) Pathogenesis of demyelination induced by a mouse hepatitis virus (JHM virus). Arch Neurol 28:298–303

Weiner LP, Johnson RT, Herndon RM (1973) Viral infections and demyelinating diseases. New Engl J Med 288:1103–1110

Wisniewski HM (1977) Immunopathology of demyelination in autoimmune diseases and virus infections. Br Med Bull 33: 54–59

Received October 27, 1982/Accepted March 8, 1983